

## The Effect of Polyethylene Crystallinity and Polarity on Thermal Stability and Controlled Release of Essential Oils in Antimicrobial Films

Roni Efrati,<sup>1</sup> Michal Natan,<sup>2</sup> Avishay Pelah,<sup>1</sup> Anina Haberer,<sup>2</sup> Ehud Banin,<sup>2</sup> Ana Dotan,<sup>1</sup> Amos Ophir<sup>1</sup>

<sup>1</sup>Department of Plastic Engineering, Shenkar College of Engineering and Design, Ramat Gan 52526, Israel

<sup>2</sup>The Mina and Everard Goodman Faculty of Life Sciences, The Institute for Advanced Materials and Nanotechnology, Bar-Ilan University, Ramat-Gan 52900, Israel

Correspondence to: R. Efrati (E-mail: ronief@gmail.com)

**ABSTRACT:** Antimicrobial packaging can preserve and increase shelf life of free preservatives food products. Active materials present in the packaging material can migrate, in a controlled manner, to the food surface, avoiding bacterial and fungal proliferation and keeping the food product edible for longer periods of time. Essential oils (EO) are natural antimicrobial agents that can be released to the headspace with no direct contact between the package and the food. To minimize losses of EO during high heat melt processing, a three stages process was implemented and tested. Antimicrobial films were prepared by melt mixing a variety of polyethylene copolymers in the presence of organo-modified montmorillonite nano clay (NC) and thymol, an EO present in oregano and thyme. A controlled EO desorption from films can be achieved by changing the polymer crystallinity and polarity. As the crystallinity increased, the thermal stability of the EO during the extrusion process improved. The addition of NC affects the structure and homogeneity of the crystals. The combination of high polymer crystallinity and chemical affinity between EO and NC increased the thermal stability of the EO during film processing, enabling to control the desorption rate. The effect of multilayer structure based on varied densities and polarities was also studied. Increasing the polarity of the outer layers in multilayered film reduced the EO desorption rate as a result of chemical interactions between the polymer and the EO. The final antimicrobial activity of the films was also found to be dependent on the EO partitioning. © 2014 Wiley Periodicals, Inc. *J. Appl. Polym. Sci.* **2014**, *131*, 40309.

**KEYWORDS:** clay; composites; crystallization; films; packaging

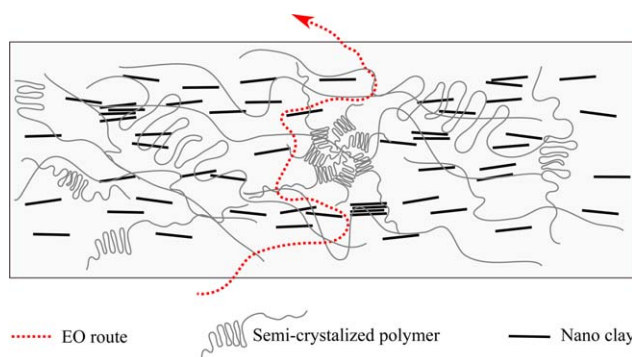
Received 12 November 2013; accepted 7 December 2013

DOI: 10.1002/app.40309

### INTRODUCTION

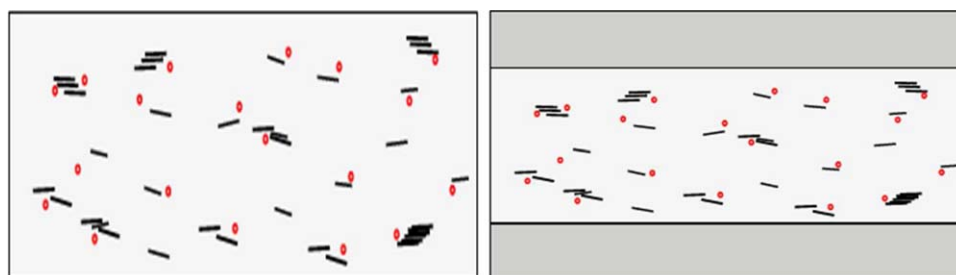
The main cause of food products deterioration with relatively high content of water and low content of fat is due to the development of bacteria and fungi.<sup>1,2</sup> Despite significant development in hygiene technology and food production, food safety is a subject that arouses great interest among the population and is still unresolved.<sup>3</sup> It has been estimated that about 30% of the people in industrialized countries suffer from a food borne disease each year.<sup>4,5</sup> Food packaging has an important role in maintaining the quality of the food with longer shelf life. Antibacterial food packaging are not just a passive barrier to physical and chemical interactions of food with the external environment, but an active system able to change the atmosphere inside the package, reduce the proliferation of bacteria and thereby increase the shelf life of the food.<sup>3,6,7</sup> In fresh or processed food, the development of bacteria occurs mainly on the food surface.<sup>8</sup> Traditionally, antimicrobial agents were added directly to the foods; and, their activity could be inhibited as a

result of interaction between preservatives and nutrients in the food, decreasing the effectiveness. For these cases, antibacterial packaging can be more effective.<sup>3,9</sup> This activity could be achieved by either indirect contact between the antimicrobial package and the food using volatiles active products or by direct contact between the antimicrobial package and the food using nonvolatiles antimicrobial systems.<sup>6,10,11</sup> The volatiles antimicrobial systems offer an advantage for high surface food products such as dry goods, fruit and vegetables.<sup>9</sup> EOs attract attention as natural materials that can substitute synthetic preservatives for fresh and processed food.<sup>1,4</sup> Thymol is an EO present in various plants, including oregano and thymes.<sup>4,12</sup> Thymol is a hydrophobic phenol with proofed activity against the proliferation of different bacteria (*Escherchia coli*, *Salmonella typhimurium*, *Staphylococcus aureus*, *Listeria monocytogenes*, and *Bacillus cereus*),<sup>4</sup> yeast (*Candida albicans*), and molds (*Aspergillus flavus* or *Penicillium nalgiovense*).<sup>13</sup> Various attempts have been made to integrate thymol in antibacterial films for food packaging



**Figure 1.** Illustration of the diffusion of penetrates through partially intercalated and exfoliated nanocomposites based on semicrystalline polymer. [Color figure can be viewed in the online issue, which is available at [wileyonlinelibrary.com](http://wileyonlinelibrary.com).]

applications.<sup>3,10,11,13–17</sup> One of the challenges in adding EOs as active substances is their high volatility. This high volatility may be an obstacle when it comes to high temperature processing of films. To overcome this challenge, nanoparticles can be used to control adsorption and desorption of the volatile active substances. Nanoparticles can affect the mass transfer properties of the film, chemically, by increasing the affinity between system components, and physically, by creating barriers which extend the route of the EO molecules path through the polymer matrix.<sup>9</sup> Nano clays (NCs) are being implemented and tested in different polymers to improve mechanical and barrier properties of polymers for packaging purposes.<sup>18–20</sup> In addition to these properties, it was found that chemical treated NCs can have higher adsorption capacity, depending on chemical moieties used.<sup>21</sup> Clay minerals have been modified with quaternary amine cations, replacing the exchangeable inorganic sodium, potassium, or calcium ions on the clay surface. The chemical treatment changes the hydrophilic nature into hydrophobic, and increases the distance between the galleries of which the clays are consisted.<sup>21</sup> Polymer density and its degree of crystallinity can also affect the diffusion kinetics. It can be assumed that increasing the degree of crystallinity, the tortuous path is increased and therefore the diffusion is slower.<sup>22</sup> Crystals are impermeable<sup>22</sup> and cannot absorb the EO. In the impregnation stage, a higher crystallinity can lead to a decrease in absorption rate. However, when considering desorption out of the film, higher crystallinity offers a better barrier for EO molecules (Figure 1).



**Figure 2.** Single layer and multilayer antimicrobial nanocomposite films proposed. [Color figure can be viewed in the online issue, which is available at [wileyonlinelibrary.com](http://wileyonlinelibrary.com).]

Chemical affinity has also great influence on EO sorption, diffusion and desorption.<sup>23</sup> High sorption and diffusion rate are obtained when there is high chemical affinity between the polymers and penetrate. This affinity can reduce penetrate desorption rate enabling the control of the migration.<sup>11</sup> The main purpose of this work is to study the effects of different polymers with different polarities and crystallinity degrees in single and multilayered nanocomposite films on the EO carrying capacity and migration kinetics (Figure 2).

## EXPERIMENTAL

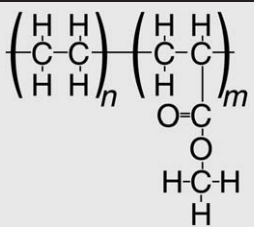
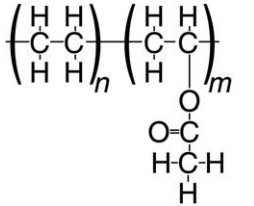
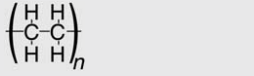

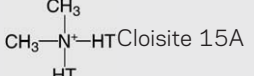
### Materials

The main polymer material used in this study was a linear low density polyethylene (LLDPE) LL-118 grade of BRASKEM, having melt flow index (MFI) of  $1.0 \text{ g } 10 \text{ min}^{-1}$ , and density of  $0.916 \text{ g cm}^{-3}$ . To understand the influence of the polymer density and crystallinity on the EO absorption and desorption properties, two additional polyethylenes were used: MDPE - MarFlex® HHM TR 130, MFI of  $0.3 \text{ g } 10 \text{ min}^{-1}$  and density of  $0.937 \text{ g cm}^{-3}$  and mLLDPE - Affinity 1880G, MFI of  $1.0 \text{ g } 10 \text{ min}^{-1}$ , and density of  $0.902 \text{ g cm}^{-3}$ . For the study of the influence of polarity and chemical affinity between the different components in multilayered film systems on the EO absorption and desorption kinetics, three additional polymers were used: Escorene Ultra FL 00209-Ethylene vinyl acetate copolymer resin (MFI of  $2.1 \text{ g } 10 \text{ min}^{-1}$ , density of  $0.931 \text{ g cm}^{-3}$  and vinyl acetate content of 9.4% wt), Cynpol EVA 0218-Ethylene vinyl acetate copolymer resin (MFI of  $2.0 \text{ g } 10 \text{ min}^{-1}$ , density of  $0.938 \text{ g cm}^{-3}$ , and vinyl acetate content of 18% wt), and DuPont™ Elvaloy® AC 1820 with 20 wt % Methyl Acrylate comonomer content (MFI of  $8 \text{ g } 10 \text{ min}^{-1}$ , and density of  $0.942 \text{ g cm}^{-3}$ ). Thymol (99.5%) was purchased from Sigma-Aldrich (Israel). Also PE-g-MAH Bondyram-4108 purchased from Polyram, Israel and TRACEL PO 2201 of Tramaco have been used, respectively, as compatibilizing and foaming agents. The organically modified clay Cloisite 15A based on dimethyl, dehydrogenated tallow, (DMDT-MMT) was supplied by Southern Clay Products/Rockwood Additives (dried in vacuum oven at  $110^\circ\text{C}$  overnight before use in melt processing; Table I).

### Sample Preparation

Different formulations were obtained using three stages processing with the purpose of minimizing loss of active substance during thermal processing: (i) first of all, a master batch was produced by melt blending in a twin screw extruder at  $230^\circ\text{C}$ , 250 rpm. Different concentrations of NCs and foaming agents

**Table I.** Chemical Structure of the Materials Used

| Material name and shortcut   | Chemical structure   |
|------------------------------|--|
| Ethylene Methyl Acrylate-EMA |   |
| Ethylene vinyl acetate-EVA   |   |
| Polyethylene (PE)            |   |
| Thymol EO                    |   |
| CLOISITE 15A-NC              | <br>where HT is Hydrogenated Tallow (~65% C18; ~30% C16; ~5% C14) |

were introduced with polymer and compatibilizer. (ii) The absorption of EO by the foamed pellets was done by mixing the pellets with EO in a closed tank at 70°C for 24 h. (iii) Antimicrobial films were produced by dry mixing the EO containing master batches with neat polymer in a cast extrusion machine at 230°C. Films with single layer based on three different polymer densities and six different multilayer films were produced. Samples without active ingredient were also prepared for control. The average thickness of the films was ~100  $\mu\text{m}$ .

### Material Characterization

The active films were characterized using different techniques to investigate their ability to absorb and control the release of EO from the film. The thermal and antimicrobial properties of the films were studied as well.

**Quantitative Analysis of EO Concentration in the Film.** The amount of thymol in the samples was determined by UV-visible spectroscopy. The films were cut into small pieces and immersed in 2-propanol (1 mL 2-propanol for every 20 mg of film). Thymol was extracted by refluxing for 60 min. To 100 mL volumetric flasks containing 10 mL of a Standard Buffer Solution (Boric Acid + Potassium Chloride, 0.2M), 1 mL of Chlorimide solution (Gibbs reagent), 4 mL of 2-propanol, and 1 mL of the extraction solution was added. After gentle mixing, the solution turned blue as a result of the chemical reaction between thymol and the Gibbs reagent. The reaction mixture

was allowed to stand for 15 min, after which distilled water was added to the volumetric flasks making up a 100 mL solution. The absorbance of the various solutions was measured at  $\lambda = 590 \text{ nm}$ , using a UV-visible 1650PC spectrophotometer, Shimadzu. Thymol content was then calculated from a calibration curve.

**Migration Characterization.** The migration characterization of the active substance was done by using two different techniques; quantification of the EO in the film by extraction and UV-visible spectroscopy analysis (as explained in section “Quantitative analysis of EO concentration in the film”) and by headspace analysis, using an auto sampler headspace GC-MS. GC-MS analysis was used to evaluate the EO concentrations as a function of time in the headspace using a Thermo GC-MS system (Finnigan Trace GC ultra, Finnigan Trace DSQ) equipped with HTA HT200H headspace auto sampler; RESTEK column, RTX-5MS Phase. Column length was 30 m, an inner diameter of 0.25 mm and a film thickness of 0.25  $\mu\text{m}$ . Each sample was held in the auto sampler conditioning oven for incubation in 40°C for 2 min before 0.5  $\mu\text{L}$  injected. The GC temperature profile was initial temperature was 100°C, ramped to 200°C at 15°/min for a total run time of 8.17 min; 50 mm<sup>2</sup> film samples were incubated in 20 mL headspace vials for 2 min at 40°C before extraction. Quantification of EO was carried out using a calibration curve.

**Thermal Analysis.** Melting temperature ( $T_m$ ) and heat of fusion ( $\Delta H_m$ ) were obtained from the DSC thermograms. DSC tests were conducted by using a TA DSC TA Q-2000 instrument (New Castle, DE) 8 mg of films were introduced in aluminum pans (40  $\mu\text{L}$ ) and were submitted to the following thermal program: heating from 23 to 150°C at 10°C min<sup>-1</sup> (2 min hold), cooling at 10°C min<sup>-1</sup> to 23°C (2 min hold) and heating to 150 at 10°C min<sup>-1</sup>.

**FTIR-Fourier Transform Infrared Spectroscopy.** The interactions between thymol and polymers were analyzed by Fourier Transform Infrared Spectroscopy-FTIR spectroscopy (ALPHA BRUKER).

**Solubility Parameter Analysis using Hansen Solubility Parameters in Practice (HSPiP) Software.** The solubility parameters of the film components (polymers, nanoclays, and thymol) were calculated using a computer program HSPiP software (<http://www.hansen-solubility.com>).<sup>24</sup> This program (HSPiP v4) allows assessing the level of interactivity between the materials. The program takes into account all types of interaction; dispersion forces, polar forces, and hydrogen bonds, which can take place between two different materials. The program was used to plot the polymers in a form of a 3D-sphere. Thymol was spatially located in the polymer sphere and the RED number (relative energy difference) could be calculated. The RED number can help to predict and understand the theoretical chemical affinity between the materials in the films and predict desorption kinetics.

**Antimicrobial Activity of the Films.** The antibacterial activity of the various films was evaluated and compared with both untreated bacteria using *E. coli* ATCC 8739 as the experimental model and to a reference Polyethylene control film. *E. coli* bacteria were grown over night in Nutrient Broth (NB, Sigma)

**Table II.** Samples Composition

|    | Sample Name        | NC wt % | FA wt % | PE-g-MAH wt % | LLDPE wt % | EO wt % in the active layer | Number of layers | Outer layer |
|----|--------------------|---------|---------|---------------|------------|-----------------------------|------------------|-------------|
| 1  | VLDPE              | 5       | 0       | 5             | 87         | 3                           | 1                | -           |
| 2  | LLDPE              | 5       | 0       | 5             | 87         | 3                           | 1                | -           |
| 3  | MDPE               | 5       | 0       | 5             | 87         | 3                           | 1                | -           |
| 4  | 3LEVA9             | 10      | 1.3     | 5             | 80.7       | 3                           | 3                | EVA9        |
| 5  | 3LEVA18            | 10      | 1.3     | 5             | 80.7       | 3                           | 3                | EVA18       |
| 6  | 3LEMA              | 10      | 1.3     | 5             | 80.7       | 3                           | 3                | EMA         |
| 7  | 3LVLD              | 10      | 1.3     | 5             | 80.7       | 3                           | 3                | VLD         |
| 8  | 3LLLD              | 10      | 1.3     | 5             | 80.7       | 3                           | 3                | LD          |
| 9  | 3LMD               | 10      | 1.3     | 5             | 80.7       | 3                           | 3                | MD          |
| 10 | Mono layer (LLDPE) | 10      | 1.3     | 5             | 80.7       | 3                           | 1                | -           |

media under shaking (250 rpm) at 37°C. In the following day, the overnight culture was diluted in a fresh NB medium to OD = 0.1, which approximately corresponds to 10<sup>8</sup> colony forming units (CFU) per mL, and grown for 1.5 h to allow the cells to enter a logarithmic state until OD = 0.6 was reached. Then, the bacteria were diluted into NB 1% (1 : 100) to obtain a stock solution with a working concentration of 10<sup>5</sup> CFU/mL; 3 mL from the stock solution were taken into each well in a 6-well plate (DE-GROOTH). Each of the various films was laid on top of the well in a way that there was no direct contact between the film and the bacterial solution, thus the antibacterial activity if achieved would be due to the migration of the oil from the film to the bacterial solution. In light of the oil's evaporation, there was a separation between the films, thus each plate received one film and the empty wells were filled with an equal volume of water. The plates were then incubated on a shaker (100 rpm) at 37°C for 20–24 h. In the day after, serial dilutions were carried out and the cells were spotted onto NB agar plates. The NB plates were incubated at 37°C for 20 h. Cell growth was monitored and determined by viable cell count.

**Film Composition.** Samples names in Table II denote the film composition. This research was divided in two parts, in the first part, (samples 1–3) nano composites based on polymers with different levels of crystallinity were studied, and in this study, the name of the sample denotes the density of the polymer. Samples 4–10 are related to the second part, the study of the influence of the outer layer in a multilayered film. In this study, samples names were determined as follows: “3L” for three layers, the other letters represents the polymer at the outer layer

**Table III.** % of Initial EO (3% wt) Left After Processing in Single Layer Antimicrobial Film with Different Polymer Densities

| Film sample | % of initial EO (3% wt) left after processing |
|-------------|---|
| VLDPE       | 52.80%  |
| LLDPE       | 63.60%  |
| MDPE        | 81.40%  |

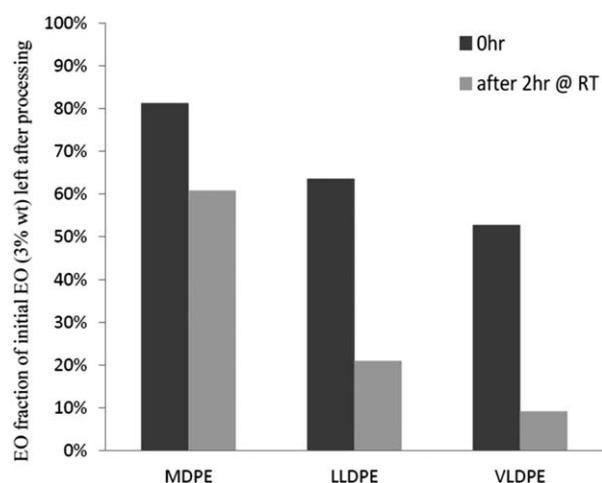
of the film- “EVA9” for ethylene vinyl acetate copolymer with vinyl acetate content of 9.4 wt %, “EVA19” for ethylene vinyl acetate copolymer with vinyl acetate content of 19 wt %, etc. Sample 10 is a mono layer film, for comparison purposes.

## RESULTS AND DISCUSSION

### Quantitative Analysis of EO Concentration in the Film

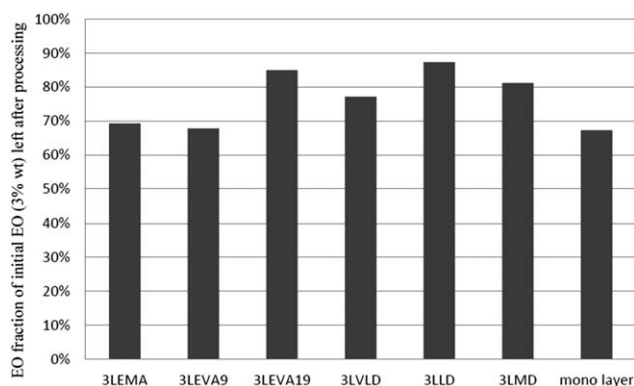
Cast extrusion was done at 230°C. This temperature may lead to a severe evaporation of the EO, which can be reduced according to the composition of the film. It could be noticed that as the polymer density increased, less EO evaporated during processing. The nominal concentration of the EO in the film was 3 wt %. However, the final concentrations were dependent on the ability of the film to delay EO desorption due to tortuosity or polarity. As one can see in Table III and Figure 3, the polymer density has an influence on the ability of the film to protect the EO during processing.

Results of EO concentration in multilayered film compared to the concentration before processing are shown in Table IV and Figure 4. The initial concentration of the EO in the active

**Figure 3.** EO concentration in the film after processing for varying polymer densities. % of initial EO (3% wt) left after processing.

**Table IV.** EO Concentration in the Film After Production Compared Concentration Before Processing in Multilayered Film with Different Outer Layers

| Film sample | EO concentration in the film vs. EO before processing |
|-------------|---|
| 3LEMA       | 69.30%  |
| 3LEVA9      | 67.80%  |
| 3LEVA18     | 85.00%  |
| 3LVLDPE     | 77.10%  |
| 3LLDPE      | 87.40%  |
| 3LMDPE      | 81.20%  |
| Mono layer  | 67.30%  |

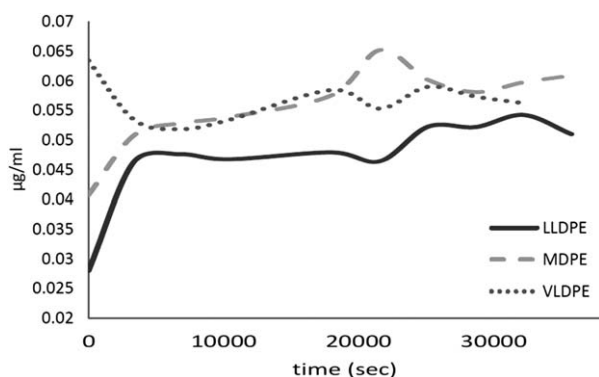


**Figure 4.** EO fraction of initial EO (3% wt) left after processing—in polymers with different outer layers in multilayered films.

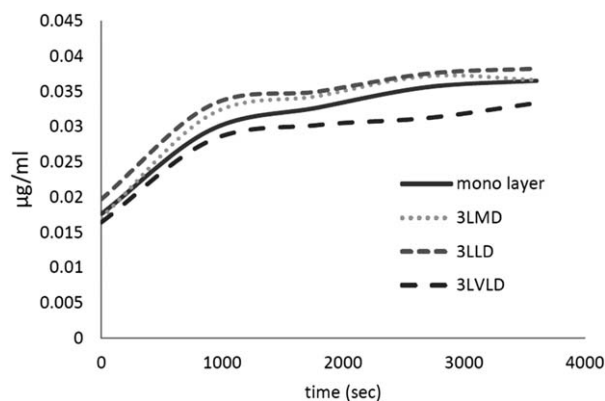
(middle) layer of each film was 3 wt %, no EO was added to the outer layers and their role was delay desorption during processing. As one can see EVA18 and LLDPE have shown ability to delay desorption during processing.

#### Migration Characterization

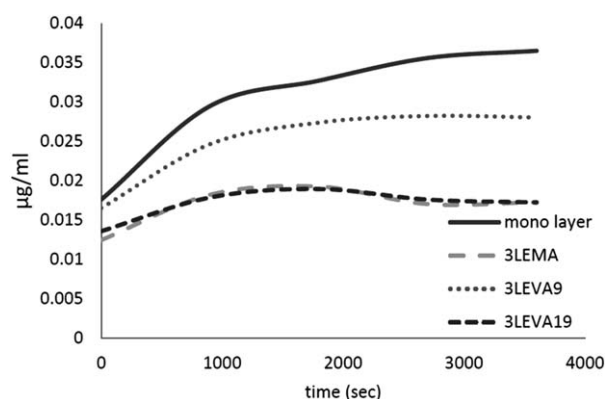
Migration depends upon the conditions in which the test is being performed and on the type of media the migration occurs in (different simulants,<sup>11</sup> air, etc). Volatile antimicrobial substances, such as EO, can act on foodstuff without direct contact, through migration of EO molecules to the headspace of the



**Figure 5.** EO headspace concentration vs. time for polymers with different levels of density/crystallinity.

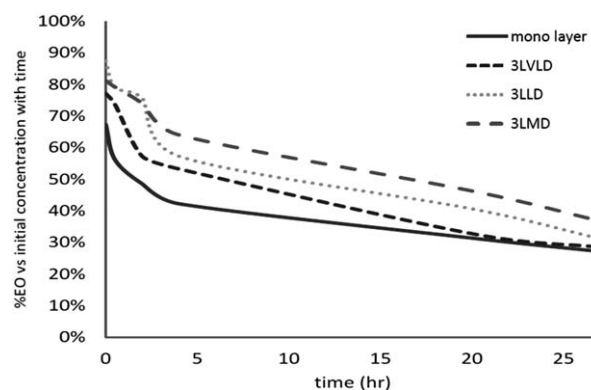


**Figure 6.** EO headspace concentration vs. time for multi layered antimicrobial films with different polymer densities in the outer layer.

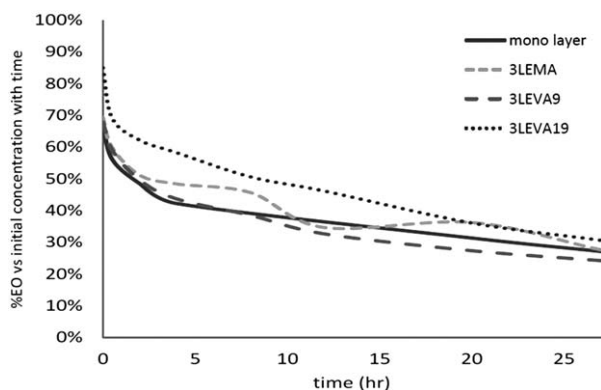


**Figure 7.** EO headspace concentration vs. time for multilayered antimicrobial film with different polymer polarities in the outer layer.

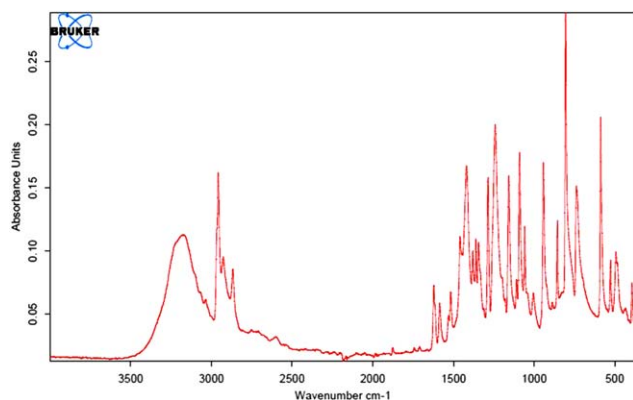
package. For this reason, it is of great importance the determination of the concentration of the active compound in the headspace. In an open container, the large osmotic pressure gradient will result in fast migration. However, when stored in a closed container the migration rate will be reduced and limited by the state of equilibrium and partitioning. For this reason, two different tests were performed. First, the amount of EO in films exposed to air for different periods of times was measured (Figures 8 and 9) using extraction and colorimetric test. In the



**Figure 8.** The influence of outer layer density on EO migration.



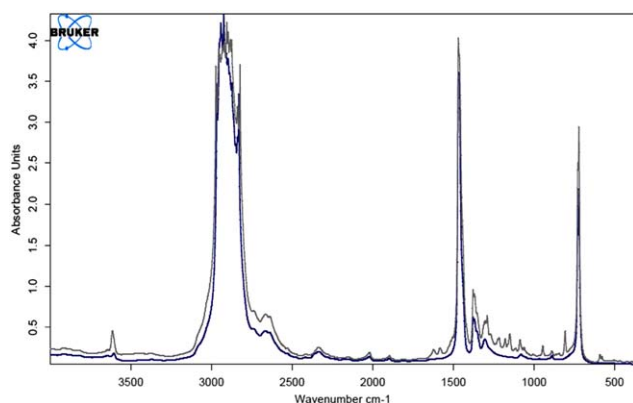
**Figure 9.** The influence of outer layer polarity on EO migration.



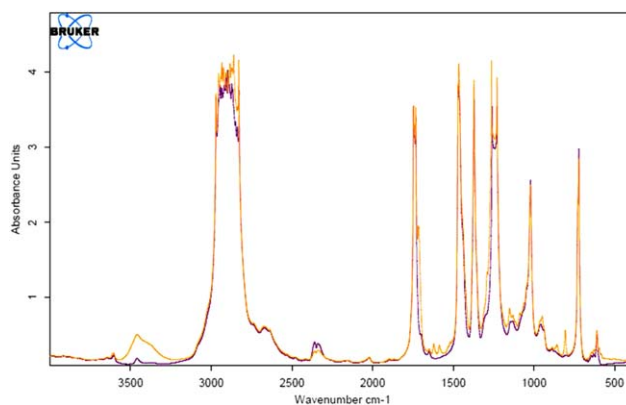
**Figure 10.** ATR thymol spectrum. [Color figure can be viewed in the online issue, which is available at [wileyonlinelibrary.com](http://wileyonlinelibrary.com).]

second test, the amount of EO released to the headspace of a closed glass vial was evaluated by an auto sampler headspace GC-MS (Figures 5–7). In this test, the vials with samples were kept at room temperature, and the conditioning time of each sample was 2 min at 40°C.

As can be seen in Figure 5, the EO migrates very fast from VLDPE. However, samples with a higher density and higher crystallinity (LLDPE and MDPE) show a delay in EO desorption



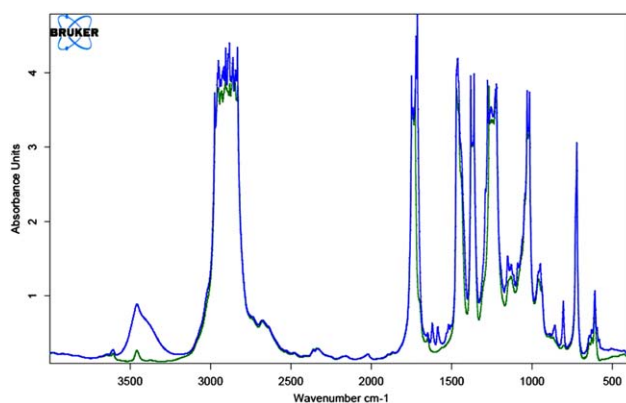
**Figure 11.** FTIR spectra of LDPE with EO (blue) and without EO (gray). [Color figure can be viewed in the online issue, which is available at [wileyonlinelibrary.com](http://wileyonlinelibrary.com).]



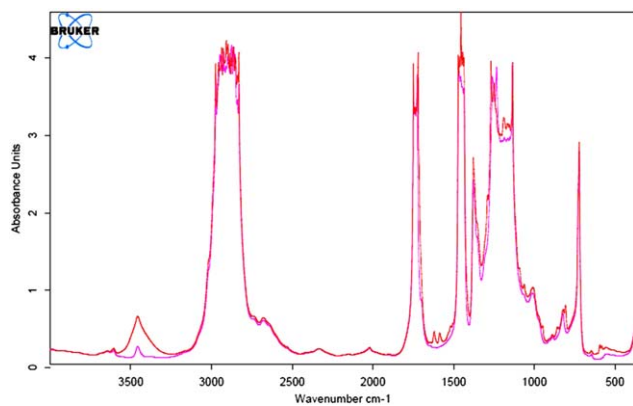
**Figure 12.** FTIR spectra of EVA-9 with EO (orange) and without EO (purple). [Color figure can be viewed in the online issue, which is available at [wileyonlinelibrary.com](http://wileyonlinelibrary.com).]

leading to the conclusion that the polymer crystals create a high tortuosity resulting in a barrier for the EO migration.

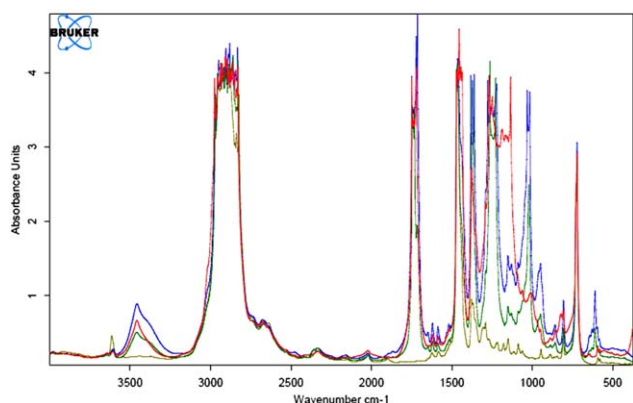
Figures 6 and 7 depict the outer layer influence on the EO desorption from multilayer films. In Figure 6, the outer layers are built from polymers with different densities. No significant effect on the EO desorption could be noticed. The effect of outer layer density on desorption to air at room temperature can be seen in Figure 8. The crystallinity degree affects the ability of the film to hold the EO. As the crystallinity is higher, the ability to hold the EO for longer periods of time increases. In Figure 7 the outer layers are based on polymers with different polarities. These results are correlated with the results shown in Figure 9; EVA18 has shown greater ability to control the EO release. The shape of the curve obtained depends on various coefficients affecting the diffusion predicted by various models. According to diffusion models, diffusion coefficient affects the diffusion rate until the equilibrium, while the partition coefficient affects the equilibrium concentration in the headspace.<sup>25</sup> Cran et al.<sup>11</sup> studied the migration of EO from LDPE containing 0, 10, and 50% (w/w) EVA. EVA has shown two opposite effects. However, it increased the affinity between the polymer matrix and the EO



**Figure 13.** FTIR spectra of EVA-19 with EO (blue) and without EO (green). [Color figure can be viewed in the online issue, which is available at [wileyonlinelibrary.com](http://wileyonlinelibrary.com).]



**Figure 14.** FTIR spectra of EMA with EO (red) and without EO (pink). [Color figure can be viewed in the online issue, which is available at [wileyonlinelibrary.com](http://wileyonlinelibrary.com).]



**Figure 15.** FTIR spectra of different polymers with thymol EO: EMA (red), EVA-9 (green), and EVA-19 (blue), LDPE (khaki). [Color figure can be viewed in the online issue, which is available at [wileyonlinelibrary.com](http://wileyonlinelibrary.com).]

causing a desorption delay, and however, it reduced the crystallinity, accelerating desorption. In this study, no reduction of crystallinity could be noticed, since the layer containing EO did not contain EVA. It could be noticed that the polarity has a significant influence on the EO desorption, the change in curve shape represents the ratio of the migrant concentration

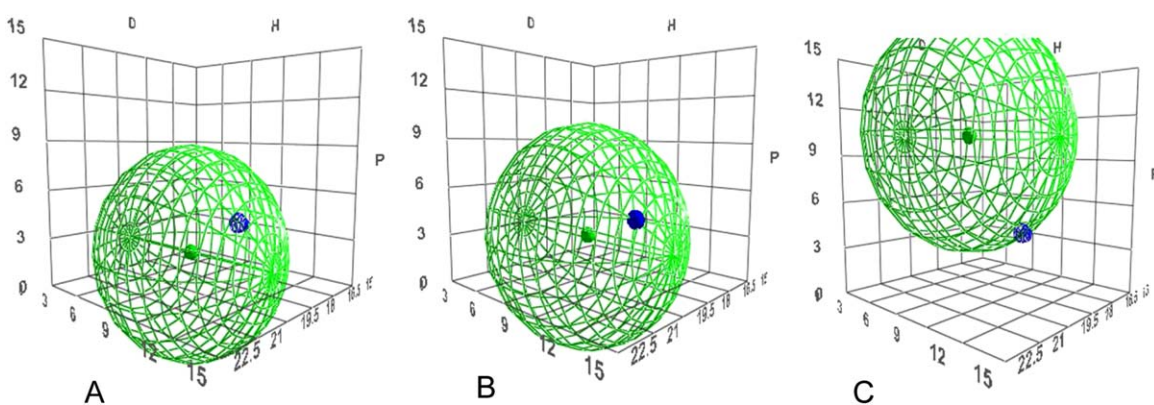
**Table V.** Solubility Parameters of the Materials in the Study and RED Number of the Thymol in Different Polymers According to HSPiP

| Polymer      | $\delta D$ | $\Delta P$ | $\delta H$ | $\Delta$ Total<br>(cal/cm <sup>3</sup> ) <sup>0.5</sup> | RED  |
|--------------|------------|------------|------------|---|------|
| PE           | 16.90      | 0.80       | 2.80       | 8.38  | 1.22 |
| PVA          | 17.60      | 2.20       | 4.00       | 8.89  | 0.96 |
| EVA9         |            |            |            | 8.43  |      |
| EVA18        |            |            |            | 8.47  |      |
| PMMA         | 18.60      | 10.50      | 5.10       | 10.73   | 1.04 |
| EMA18        |            |            |            | 8.80  |      |
| Thymol       | 19.00      | 4.50       | 10.80      | 10.91   |      |
| Cloisite 15A | 18.20      | 3.80       | 1.70       | 9.13  |      |

in the packaging to the migrant concentration in the food simulant at equilibrium, which reflects the effect in partition coefficient.<sup>25</sup> An attempt to use diffusion model based on Crank model<sup>26</sup> showed that there is a large gap between the empirical results obtained and the model.

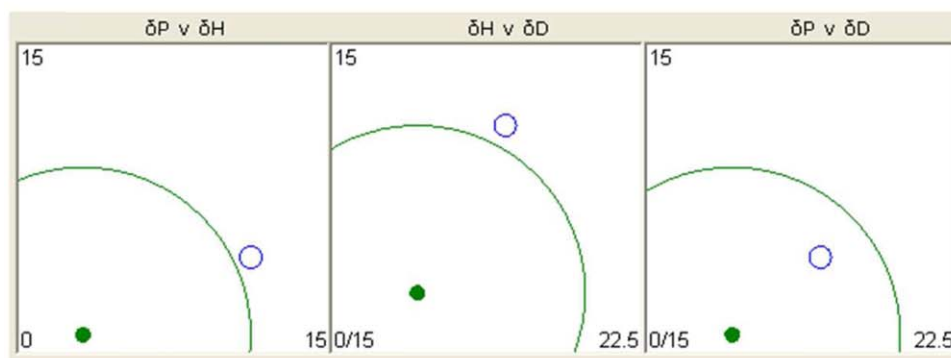
#### Polymer-EO Interactions

**FTIR.** The IR spectrum of neat thymol and compounds with thymol are presented in Figures 10–15. The most intense peaks at 738 and 807 cm<sup>-1</sup> are assigned to ring vibrations of the thymol chemistry.<sup>15</sup> The peaks around 3400 cm<sup>-1</sup> are assigned to hydrogen bonds, free hydrogen bonds are narrower as compared with peaks of bonded hydrogen bonds and can be seen at higher wavelength (3580–3650 cm<sup>-1</sup> and 3200–3550 cm<sup>-1</sup>, respectively). Figures 12–14 depict the increase in hydrogen bond peaks at 3450 cm<sup>-1</sup> as a result of thymol affinity to the polar polymers EVA9, EVA18, and EMA18, this peak was not found in Figure 11 (PE spectra with and without EO). In Figure 15, different polymers with EO spectra are shown. The hydrogen bonds peak around 3450 cm<sup>-1</sup> represent the interaction of thymol and the polymers. When comparing the copolymers EVA9 and EVA18, the main difference between them is the polar comonomer percentage. As the polar comonomer percentage increases the interaction between the polymer and the EO become stronger. In addition, when comparing two copolymers

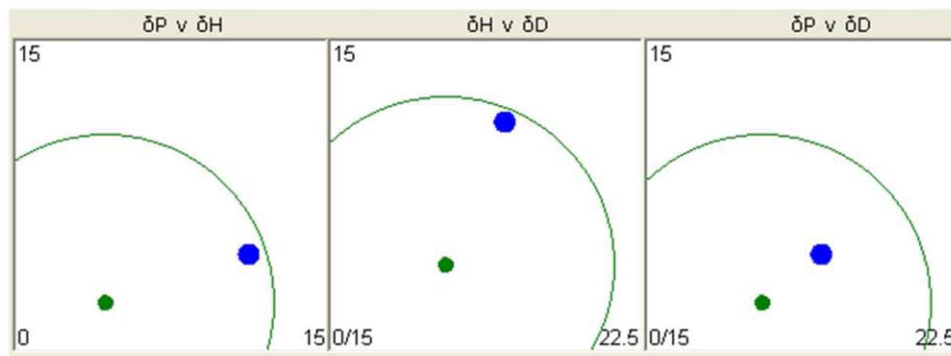


**Figure 16.** 3D plot of the data for Polyethylene (A), Polyvinyl acetate PVA (B), and Poly butyl acrylate PMMA (C), represented by the green sphere. The blue dots are the thymol EO. [Color figure can be viewed in the online issue, which is available at [wileyonlinelibrary.com](http://wileyonlinelibrary.com).]

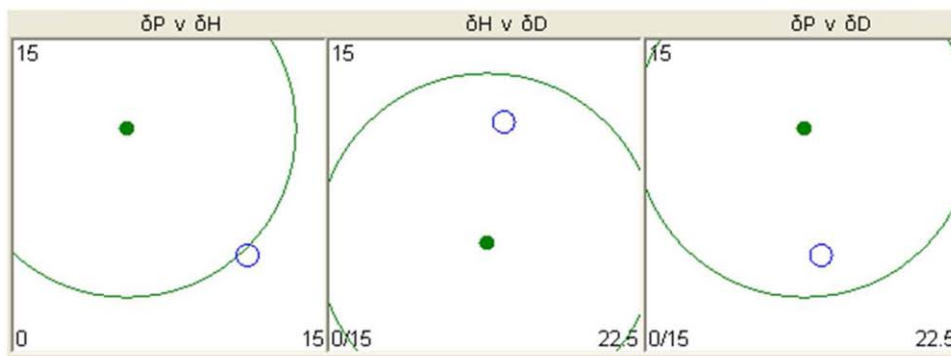
## A-Polyethylene



## B- Polyvinyl acetate PVA



## C- Poly methyl methacrylate PMMA



**Figure 17.** 2D plot of the data for Polyethylene (A), Polyvinyl acetate PVA (B), and Polymethyl methacrylate PMMA (C), represented by the green sphere. The blue dots are the thymol EO. [Color figure can be viewed in the online issue, which is available at [wileyonlinelibrary.com](http://wileyonlinelibrary.com).]

with different interactive group and the same percentage of polar comonomer group, EVA18 and EMA18, the functional group influences the degree of interaction of the polymer with the EO. The interaction between EVA18 and the EO is stronger than that of EMA18. As a result; as the outer layer polymer is more polar, the desorption rate is slower due to strong interactions.

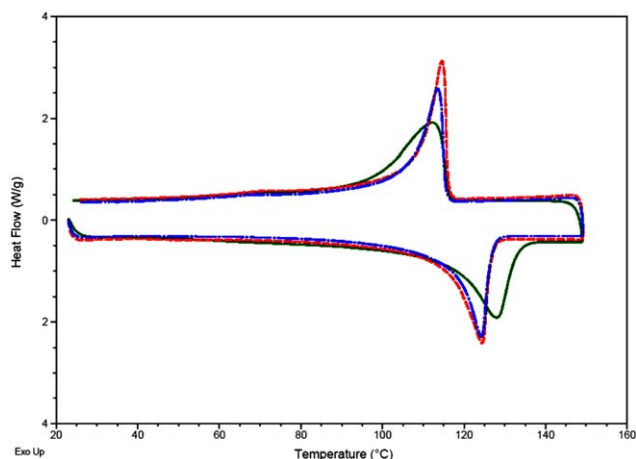
**Hansen Solubility Parameters.** HSPiP software is a convenient and simple tool that allows the prediction of interactions between different materials by using the solubility parameters and interactions of the components. Solubility parameter is a thermodynamic property derived from cohesion energy that can help to predict

the ability of different components in a system to interact with each other.<sup>27</sup> The solubility parameters of the materials can be seen in Table V. The solubility parameters of the copolymers EMA18, EVA18, and EVA9 were calculated using the law of mixture [eq. (1)], while the solubility parameters of the co-monomers are taken from HSPiP software, PMMA was the model to examine PMA properties, since both have the same interactive groups.

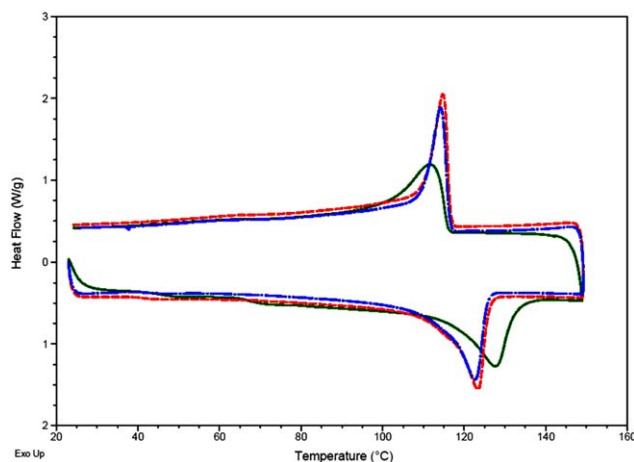
$$X_c = X_m V_m + X_f V_f \quad (1)$$

The solubility parameter gap the “difference” ( $\Delta\delta$ ) of two materials can be calculated in different ways. The equation used in HSPiP software takes into account the contribution





**Figure 18.** Neat MDPE (green line) compared with composite film with EO (blue line) and without EO (red line). [Color figure can be viewed in the online issue, which is available at [wileyonlinelibrary.com](http://wileyonlinelibrary.com).]



**Figure 19.** Neat LDPE (green line) compared with composite film with EO (blue line) and without EO (red line). [Color figure can be viewed in the online issue, which is available at [wileyonlinelibrary.com](http://wileyonlinelibrary.com).]

of dispersion, polar and hydrogen-bonding interactions [eq. (2)].

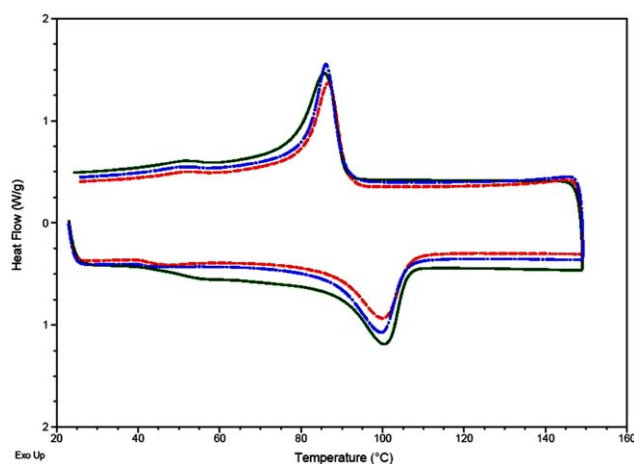
$$\begin{aligned} (\text{Difference})^2 = \Delta\delta^2 = & 4(\delta D_A - \delta D_B)^2 \\ & + (\delta P_A - \delta P_B)^2 + (\delta H_A - \delta H_B) \end{aligned} \quad (2)$$

The green dot inside the sphere in Figures 16 and 17 represents the solubility parameters ( $\delta D$ ,  $\delta P$ , and  $\delta H$ ) of a particular polymer. The blue dots represent the thymol. The RED (relative energy difference) number and the location of the blue dot in relation to the green sphere indicate the miscibility between thymol and the polymers. If the blue dots are solid, the thymol is located inside the polymer sphere and the RED number is  $<1$ , indicating good affinity between polymer and thymol. If the blue dots are open, the thymol is outside the polymer sphere in all planes (one or two inside and one or two outside the radius), and the RED number is  $>1$  indicating low affinity between polymer and thymol.

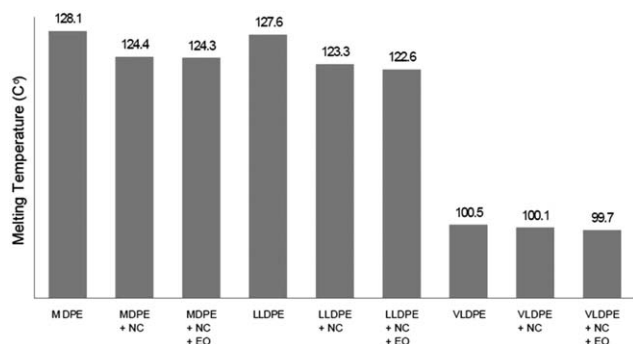
As can be seen in Table V, the solubility parameter difference,  $\Delta\delta$ , between the EO and the relevant polymers (PE, EVA9, EVA18, and EMA18) is quite similar [between 1.42 and 1.84 (cal/cm<sup>3</sup>)<sup>0.5</sup>]. However, the type of interactions that might occur with the various polymers can differ, as can also be seen in Figures 16 and 17. While polyethylene lead to dispersion forces based on Van der Waals interactions only, polar polymers like PMA and PVA can lead to interactions based on polar forces and even hydrogen bonds (as shown in the FTIR figures), which are able to overcome the gap in solubility parameters of the components. According to Camacho et al.,<sup>27</sup> the solubility parameters of EVA with different vinyl acetate content is closer to the solubility parameters of pure vinyl acetate [8.99 (cal/cm<sup>3</sup>)<sup>0.5</sup> @30°C] as the vinyl acetate content increases. That means that when comparing the solubility parameters of EVA9 and EVA18, the solubility parameter of EVA18 is closer than to the solubility parameter of PVA. That can explain the lower desorption rate properties of 3LEVA18 compare to 3LEVA9.

### Thermal Properties

Thermal properties of polymers with different crystallinity (MDPE, LLDPE, and VLDPE samples), were studied using DSC, (Figures 18–20). A comparison was made between neat polymer (green), film with NC and with EO (blue), and film with NC and without EO (red). It could be noticed from Figures 18–20 that EO has no effect on polymer crystallization temperature ( $T_c$ ).<sup>28</sup> Clay can provide heterogeneous surface increasing the crystals nucleation rate. The interfacial interactions between the surface treatment of the NCs and active groups of polymer chains can reduce molecule mobility, lowering the crystals growing rate.<sup>29</sup> In other words, the NC can act as nucleator, leading to a higher uniformity in polymer crystals shape, which can be seen by sharper melting peak. In the current study, Cloisite 15A-2M2HT: dimethyl, dehydrogenated tallow, quaternary ammonium organic modifier increased the possible interactions between the NC and the polymer molecules affecting the crystal size and leading to decrease in the



**Figure 20.** Neat VLDPE (green line) compared with composite film with EO (blue line) and without EO (red line). [Color figure can be viewed in the online issue, which is available at [wileyonlinelibrary.com](http://wileyonlinelibrary.com).]

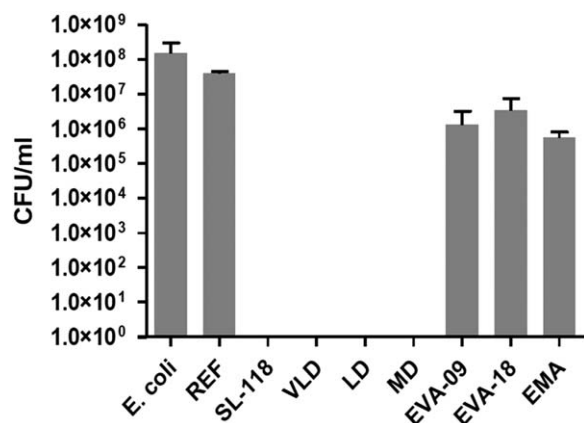


**Figure 21.** Melting temperatures of polymers and nanocomposites with and without EO.

spherulite extent, addition of NCs to MDPE and LLDPE affected the melting peak shape and crystallization peak shape from broad and small to narrow and sharp. In addition, the presence of NCs affects also the melting temperature of the polymer, as can be noticed in Figure 21. Melting temperature of MDPE and LLDPE decreased in  $\sim 4^{\circ}\text{C}$  as a result of NCs addition. In contrast, when adding NCs to VLDPE, the melting peak shape and melting temperature remained unchanged. From Figures 20 and 21, it can be seen that the NC does not influence VLDPE crystallinity. Zhang et al.<sup>30</sup> and Persico and Ambrogi<sup>9</sup> studied the addition of the nanoclay, Cloisite 20A to LLDPE and Nanomer I.28 to LDPE, respectively, and concluded that no change in the melting temperature could be noticed. However in Dabbin et al.<sup>20</sup> noticed that the addition of nanoparticles, Nanolin DK4, to a blend of LLDPE/LDPE increased the melting temperature of the polymer. Apparently, it varies according to the polymer and NC studied.

#### Antimicrobial Activity of the Films

The antimicrobial properties of the various films were tested against *E. coli*, a common food-borne bacterial pathogen. As can be seen in Figure 22, when the nonpolar polymers (VLD, LD, and MD) are at the outer layer of multilayered film, the ability of the film to inhibit bacterial proliferation is good, but when the polar polymers (EVA09, EVA18, and EMA) are at the outer layer this ability decreased. These results can be



**Figure 22.** Antibacterial activity of Thymol-containing films. *E. coli* bacteria were grown and treated with the various films as described in the experimental section.

correlated to the FTIR results that show that thymol forms hydrogen bond interactions with the polar groups of EVA and EMA, increasing the partition coefficient and leading to a low EO concentration in the headspace. This concentration is lower than the minimal concentration needed to inhibit bacterial proliferation.

#### CONCLUSIONS

The influence of polyethylene copolymers crystallinity and polarity on thermal stability and controlled release of thymol in single and multilayer antimicrobial films was studied. The films were prepared using three stage melt compounding procedure which included the addition of foaming agent and NC (Cloisite 15A). The antimicrobial active agent chosen was thymol, an EO with proved antimicrobial activity. The study on the migration behavior of thymol from the different films revealed that PE crystallinity has a considerable effect on desorption from the film surface when the oil is stored in the bulk of a single layer film structure. As the density of the polyethylene increased (higher degree of crystallinity), a higher thymol concentration was found in the film after processing. Thermal properties have showed that the partially exfoliated nanoclays dispersed in the polyethylene matrix, affect the polymer crystallization behavior. In MDPE and LLDPE, the NC addition affects both melting and crystallization peak shapes from broad and small to narrow and sharp, while in VLDPE no effect could be seen. In multilayer films the crystallinity (density) of the polyethylene showed no significant effect on desorption, even when the higher crystalline layer is the outer layer of the multilayer film. Chemical affinity between a polar PE copolymer and thymol was observed through FTIR spectroscopy (hydrogen bonds). As a result of the strong interactions, the desorption rate of the EO from the film decreased; resulting in a decrease in the antimicrobial properties of the film. Interactions between the various polar polymers and thymol differed depending on the polymer and its polar group. The antimicrobial activity of the films could be related not only to thymol concentration in the film, but also to the capability of the film to desorb EO molecules into the headspace. This understanding can enable the prediction of the potential antimicrobial film activity, based on measured desorption properties obtained by chromatography and spectroscopy techniques.

#### REFERENCES

- Kuorwel, K. K.; Cran, M. J.; Sonneveld, K.; Miltz, J.; Bigger, S. W. *J. Food Sci.* **2011**, *76*, R164.
- Duarte, S. C.; Pena, A.; Lino, C. M. *Food Microbiol.* **2010**, *27*, 187.
- Mastromatteo, M.; Danza, A.; Conte, A.; Muratore, G.; Del Nobile, M. A. *Int. J. Food Microbiol.* **2010**, *144*, 250.
- Burt, S. *Int. J. Food Microbiol.* **2004**, *94*, 223.
- Gustavsson, J.; Cederberg, C.; Sonesson, U.; van Otterdijk, R.; Meybeck, A. *Save Food! Global Food Losses and Food Waste*. Food and Agriculture Organisation: United Nations, **2011**.
- Han, J. *Food Technol.* **2003**, *54*, 56.

7. Liu, L.; Jin, T.; Finkenstadt, V.; Liu, C.-K.; Cooke, P.; Coffin, D.; Hicks, K.; Samer, C. *Chem. Chem. Technol.* **2009**, *3*, 221.
8. Ha, J.-U.; Kim, Y.-M.; Lee, D.-S. *Packag. Technol. Sci.* **2001**, *14*, 55.
9. Persico, P.; Ambrogi, V. *Polym. Eng. Sci.* **2009**, *1447–1455*.
10. Guarda, A.; Rubilar, J. F.; Miltz, J.; Galotto, M. *J. Int. J. Food Microbiol.* **2011**, *146*, 144.
11. Cran, M. J.; Rupika, L. A.; Sonneveld, K.; Miltz, J.; Bigger, S. W. *J. Food Sci.* **2010**, *75*, E126.
12. Ponce Cevallos, P. A.; Buera, M. P.; Elizalde, B. E. *J. Food Eng.* **2010**, *99*, 70.
13. López, P.; Sánchez, C.; Batlle, R.; Nerín, C. *J. Agric. Food Chem.* **2007**, *55*, 8814.
14. Ramos M.; Jiménez A.; Peltzer M.; Garrigós M. C. *J. Food Eng.* **2012**, *109*, 513.
15. Sanchez-Garcia, M. D.; Ocio, M. J.; Gimenez, E.; Lagaron, J. M. *J. Plast. Film Sheeting* **2008**, *24*, 239.
16. Corbo, M. R.; Di Giulio, S.; Conte, A.; Speranza, B.; Sinigaglia, M.; Del Nobile, M. A. *Int. J. Food Sci. Technol.* **2009**, *44*, 1553.
17. Delnobile, M.; Conte, A.; Incoronato, A.; Panza, O. *J. Food Eng.* **2008**, *89*, 57.
18. Abdollahi, M.; Rezaei, M.; Farzi, G. *J. Food Eng.* **2012**, *111*, 343.
19. Pereiradeabreu, D.; Paseirolosada, P.; Angulo, I.; Cruz, J. *Eur. Polym. J.* **2007**, *43*, 2229.
20. Dadbin, S.; Noferesti, M.; Frounchi, M. *Macromol. Symp.* **2008**, *274*, 22.
21. Adebajo, M.; Frost, R. *J. Porous Mater.* **2003**, 159–170.
22. McKeen, L. *Permeability Properties of Plastics and Elastomers*; Elsevier: USA, **2012**.
23. Massey, L. K. *Permeability Properties of Plastics and Elastomers: A guide to packaging and barrier materials*; Plastics Design Library/William Andrew Publishing, **2003**.
24. Abbott, S.; Hansen, C. M. *Hansen Solubility Parameters in Practice Complete with software, data and examples*; Hansen-Solubility, **2008**.
25. Helmroth, E.; Rijk, R.; Dekker, M.; Jongen, W. *Trends Food Sci. Technol.* **2002**, *13*, 102.
26. Vahdat, N.; Sullivan, V. D. *J. Appl. Polym. Sci.* **2001**, *79*, 1265.
27. Camacho, J.; Díez, E.; Ovejero, G.; Díaz, I. *J. Appl. Polym. Sci.* **2013**, *128*, 481.
28. Suppakul, P.; Miltz, J.; Sonneveld, K.; Bigger, S. W. *Packag. Technol. Sci.* **2006**, *19*, 259.
29. Xie, Y.; Yu, D.; Kong, J.; Fan, X.; Qiao, W. *J. Appl. Polym. Sci.* **2006**, *100*, 4004.
30. Zhang, M.; Sundararaj, U. *Macromol. Mater. Eng.* **2006**, *291*, 697.